X-ray photoemission study of the temperature-dependent CuO formation on Cu(410) using an energetic O_2 molecular beam

Michio Okada,[1,2] Luca Vattuone,[3] Kousuke Moritani,[4] Letizia Savio,[3] Yuden Teraoka,[4] Toshio Kasai,[1] and Mario Rocca[5]
[1]*Department of Chemistry, Graduate School of Science, Osaka University, 1-1 Machikaneyama-cho, Toyonaka, Osaka 560-0043, Japan*
[2]*PRESTO, Japan Science and Technology Agency, 4-1-8 Honcho, Kawaguchi, Saitama 332–0012, Japan*
[3]*Dipartimento di Fisica and CNISM Unità di Genova, Università di Genova, Via Dodecaneso 33, 16146 Genova, Italy*
[4]*Synchrotron Radiation Research Center, Japan Atomic Energy Agency, 1-1-1 Kouto, Mikazuki, Sayo, Hyogo 679-5148, Japan*
[5]*IMEM-CNR and Dipartimento di Fisica, Università di Genova, Via Dodecaneso 33, 16146 Genova, Italy*
(Received 6 March 2007; published 22 June 2007)

We studied the oxidation of Cu(410) using x-ray photoemission spectroscopy performed with synchrotron radiation. We demonstrate that a hyperthermal O_2 molecular beam is an efficient tool to fabricate Cu oxide thin films at room temperature (RT) and even lower temperatures. At RT, mainly Cu_2O forms. At $T \sim 100$ K, CuO nucleation also takes place; this is noteworthy, since this moiety is usually produced only at much higher T and ambient pressure.

DOI: 10.1103/PhysRevB.75.233413 PACS number(s): 82.65.+r, 61.80.Lj, 68.43.−h, 82.20.−w

Understanding the chemistry of the copper-oxygen interaction is one of the outstanding open issues of solid-state physics due to the obvious implications with the physics of high-T_c superconducting materials, whose basic units are Cu-O chains or layers.[1] Cuprous oxide (Cu_2O) and cupric oxide (CuO) are regarded as meaningful benchmark materials for theories and experiments. Cu_2O, an industrially important direct-gap semiconductor with a band-gap energy of 2.17 eV,[2] is expected to have an essentially full Cu $3d$ shell. On the other hand, CuO has an open d shell ($3d^9$) and is an antiferromagnetic semiconductor with a gap of about 1.4 eV.[3–5] Both materials are regarded as most promising for applications to photovoltaic cells,[6–8] for which higher carrier densities and lower leakage currents are required to improve the performance in terms of energy conversion. Finite-size effects were recently demonstrated to affect the magnetic transition temperature in CuO ultrathin films or nanoparticles.[9] Last but not the least, Cu_2O is an efficient catalyst for the partial oxidation of propylene to acrolein,[10] while CuO is used in gas sensors.[11] The synthesis of Cu_2O nanocrystals has been reported recently, further testifying the growing interest in this material.[12]

Ordered Cu_2O and CuO films and nanostructures are usually grown by controlling O_2 pressure and substrate temperature during deposition. The use of hyperthermal O_2 molecular beams (HOMBs) may improve the quality of the grown thin films, as demonstrated, e.g., for organic films,[13] and allow to produce the oxide at lower crystal temperatures, T, avoiding contamination problems and reducing film defectivity. Collision-induced absorption[14] (CIA) and local heating of the substrate were shown to be indeed effective in inducing oxide nucleation,[15] opening up other possibilities for the production of nanostructured oxides.

Herein, we report on a detailed study on the initial oxidation and on Cu_2O and CuO formation on Cu(410). The stepped surface was chosen because undercoordinated sites may act as nucleation centers and open up efficient pathways for the incorporation of O atoms[16] and because oxygen adsorption at this surface was studied thoroughly.[17] The choice of the Cu(410) geometry is further motivated by its stabilization by atomic oxygen: faceting into (410) planes of (100) surfaces was indeed reported after massive oxygen exposures.[18]

The efficiency of oxide formation increases strongly with O_2 translational energy, allowing to produce the oxide already at room temperature (RT) and even at $T \sim 100$ K for 2.2 eV O_2 beams, as demonstrated by x-ray photoemission spectroscopy (XPS) performed using synchrotron radiation (SR). The characteristic signatures of Cu_2O are then clearly visible for HOMB incidence in O $1s$ and Cu $L_3M_{4,5}M_{4,5}$ Auger spectra. At $T \sim 100$ K, additional features appear in O $1s$ and Cu $2p$ XPS spectra, witnessing CuO formation.

SR-XPS experiments were performed with the surface reaction analysis apparatus (SUREAC 2000) constructed at BL23SU in SPring-8 in Japan.[19] The photon energy for recording XPS spectra was set to 1092.8 eV. The Cu(410) sample (see schematic structure in the inset of Fig. 1) was cleaned by repeated cycles of 1 keV Ar^+ sputtering and annealing at 870 K until no impurities were detected by SR-XPS and low-energy electron diffraction showed the sharp

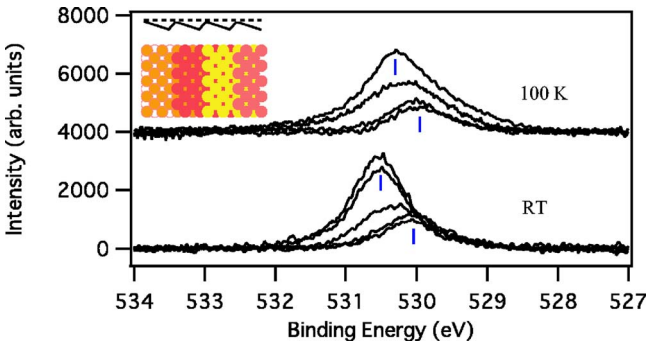

FIG. 1. (Color online) Evolution of O $1s$ SR-XPS spectra for 2.2 eV HOMB incidence along the surface normal and at room temperature (bottom) and at 100 K (top). Spectra correspond to increasing coverage from 0.5 to ~2 ML. The inset shows the Cu(410) surface geometry.

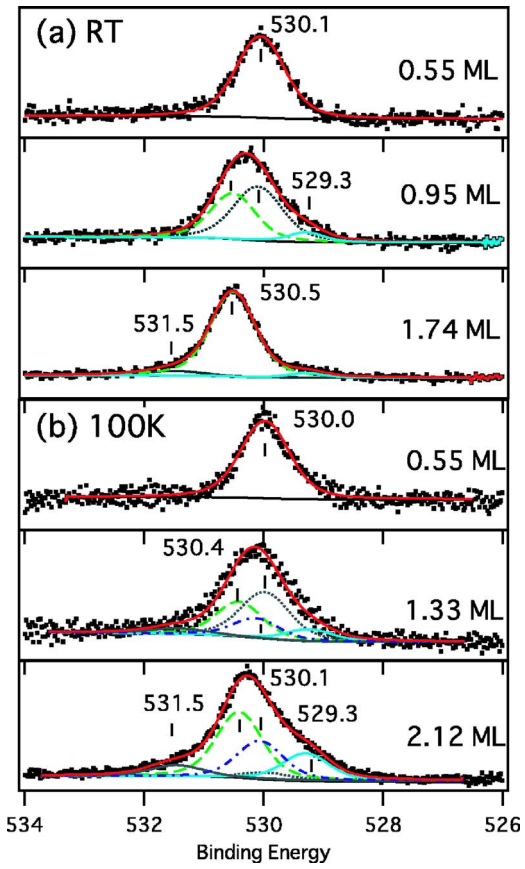

FIG. 2. (Color online) Line-shape analysis of the representative O 1*s* SR-XPS spectra at (a) room temperature and (b) $T=100$ K for 2.2 eV HOMB incidence along the surface normal. Four components are present. They correspond to chemisorbed O on Cu (530.1 eV at RT and 530.0 eV at 100 K), subsurface O (530.1 eV, only at 100 K), Cu_2O (530.5 eV), CuO (529.3 eV), and chemisorbed O on Cu oxide (531.5 eV). The Shirley background is indicated by the full line.

pattern characteristic of the pristine stepped surface. The O_2 molecules are dosed by HOMB seeded in He. Their estimated incident energy reads 2.2 eV at a nozzle temperature of 1400 K. The incident direction of the HOMB is along the normal to the sample surface. The O_2 flux at the sample position was estimated experimentally[20] to be 1.28×10^{15} molecules $cm^{-2}\,s^{-1}$, corresponding to 0.81 ML/s. [The ML is defined with respect to the unreconstructed Cu(410) substrate (1 ML$=1.58\times10^{15}$ atoms/cm^2)]. The surface coverage was determined from the area of the XPS spectra calibrated with respect to the $(2\sqrt{2}\times\sqrt{2})R45°$ structure of Cu(100).

Figure 1 shows the evolution of the O 1*s* spectral region for 2.2 eV HOMB doses performed along the surface normal at RT and $T\sim100$ K. The O 1*s* SR-XPS peak has a binding energy $E_B\cong530$ eV at a coverage of 0.5 ML, and increases in intensity and E_B with increasing O coverage at both T. However, the line shape of the O 1*s* peak depends strongly on O coverage and oxidation temperature. In Fig. 2, we show the results of the peak-shape analysis of representative O 1*s* spectra. The symmetric peak of O 1*s* at 0.55 ML at RT and ~100 K is fitted with a Voigt function with parameters Gaussian width $G=0.76$ eV and Lorentzian width $\Gamma=0.36$ eV. The peak-fitting procedure was performed using UNIFIT2002 software[21] and subtracting the Shirley background.[22] The O 1*s* binding energy reads 530.1 eV at RT (Ref. 23) and 530.0 eV at 100 K. At higher O coverage and for both T, several additional components are necessary to reproduce the measured shape, whose weight with coverage depends strongly on the oxidation temperature.

At RT, they correspond to Cu_2O ($G=0.68$ eV, $\Gamma=0.35$ eV) at 530.5 eV and to a small CuO peak ($G=0.50$ eV, $\Gamma=0.35$ eV) at 529.3 eV.[24] A small amount of CuO was also reported for Cu_2O formation on Cu(110).[25] At the highest investigated O concentration, the chemisorbed oxygen signal at 530.1 eV has disappeared, witnessing that the substrate is now fully covered by Cu_2O. The small additional peak at 531.5 eV ($G=0.87$ eV, $\Gamma=0.35$ eV) is possibly due to chemisorbed O on Cu oxide.[26]

At low T, a further peak is necessary to fit the data, corresponding to subsurface oxygen at 530.1 eV, $G=0.71$ eV, $\Gamma=0.35$ eV.[27] Although this binding energy nearly coincides with the one of chemisorbed oxygen, its introduction is justified because of the following: (1)The χ^2 value per degree of freedom decreases significantly (from 1.64 to 1.54) and the Abbe criterion coefficient, estimating the extent of systematic errors, increases from 0.84 to 0.93, indicating smaller systematic deviations (the value 1 indicates purely statistical deviations).[21]

(2) At the highest coverage, a peak at 530 eV with weight close to 0.5 ML is needed to fit the data. This coverage corresponds to the saturation of chemisorbed O. If the component at 530 eV were due only to supersurface oxygen, we should conclude that only a very small fraction of the surface is covered by oxide. The latter would then consist of three-dimensional islands unphysically elongated normally to the surface.

Cu_2O and CuO formation is confirmed by the SR-XPS Cu $L_3M_{4,5}M_{4,5}$ Auger electron spectra (AES) and by the Cu 2*p* spectra reported in Figs. 3(a) and 3(b), respectively. The reference AES spectra of bulk Cu_2O and CuO (Ref. 24) are reported in Fig. 3(a) for comparison. Cu_2O at RT can be seen in the spectral shape of the Cu $L_3M_{4,5}M_{4,5}$ AES peak of the oxidized surface. At $T\sim100$ K, the shape of the AES spectra shows, on the contrary, the larger weight of CuO and conversely the reduction of Cu_2O inferred by the O 1*s* spectra in Fig. 2. The satellite and the shoulder of Cu 2*p*, characteristic for the d^9 configuration in the ground state of CuO, are clearly present in the XPS spectra in Fig. 3(b) in the E_B range 933–945 eV for the oxidized surface prepared at $T\sim100$ K, only.

Finally, in Fig. 4(a), we show the O uptake curves recorded during 2.2 eV HOMB oxidation at RT and $T\sim100$ K. We firstly note that the uptake for Cu(410) is much faster than for the parent nonstepped Cu(100) surface [continuous line in panel (a)], thus proving the high oxidation efficiency of the low coordination sites at the steps of the Cu(410) surface. The trend is similar, except for the slightly higher coverage reached in the latter case. However, the distribution of the O 1*s* components is totally different for the two T values as it can be inferred from Figs. 2 and 4(b). At RT, the 2.2 eV HOMB produces almost only Cu_2O, while at

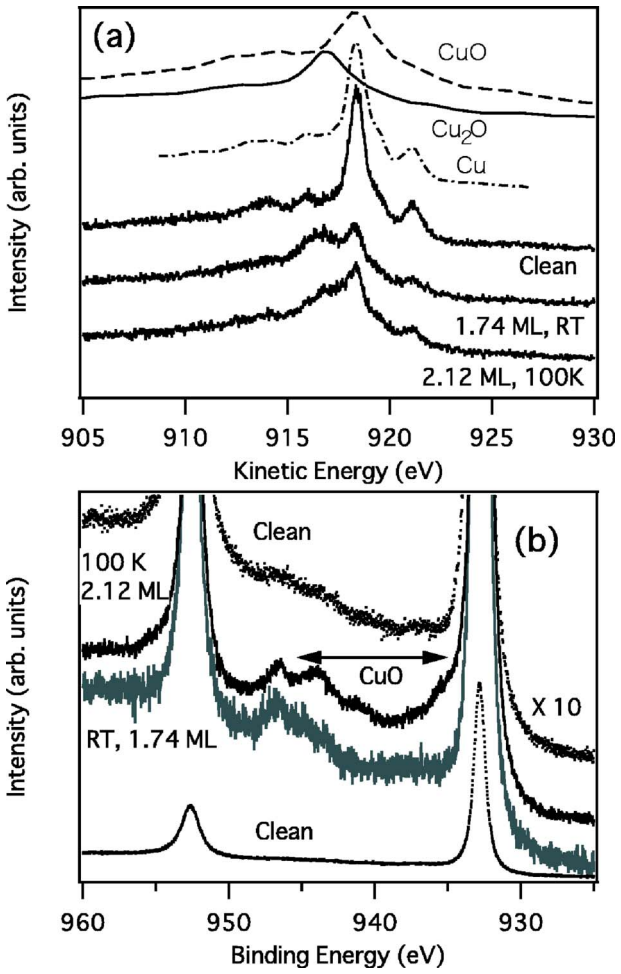

FIG. 3. (Color online) (a) Cu $L_3M_{4,5}M_{4,5}$ Auger electron spectra measured at 70° from the surface normal after 2.2 eV HOMB incidence along the surface normal. From the bottom: 2.12 ML O coverage prepared at 100 K, 1.74 ML prepared at a room temperature, and bare surface. Spectra corresponding to bulk CuO (dashed line), Cu_2O (thin line), and Cu (dot-dashed line) are also shown (Refs. 24 and 31). (b) Cu 2*p* XPS spectra measured for emission along the surface normal after 2.2 eV HOMB incidence along the surface normal. Bottom spectrum: nonmagnified spectrum of the clean surface. Enlargements (×10). From the top: clean and O covered surface (2.12 ML prepared at 100 K and 1.74 ML at RT, respectively).

$T \sim 100$ K, three phases (Cu_2O, subsurface O, and CuO) coexist. This result suggests that the local heating by HOMB is insufficient for the formation of a homogeneous Cu_2O layer. Mobility of Cu and O atoms, attained at higher T only, is thus required.

CuO nucleation at low T is anyway surprising, since this moiety is usually produced at high T and high O_2 pressure.[28,29] Cu_2O may thus form, under the present conditions, following the route of $CuO+Cu \rightarrow Cu_2O$ and the CuO phase may act as a metastable precursor. It should be noted that a similar reaction pathway, leading to Cu_2O formation, occurs when depositing Cu atoms on CuO thin films.[30] Indeed, when heating to 273 K, the O 1*s* component, corresponding to CuO, disappears in the SR-XPS O 1*s* spectrum [see Fig. 4(c)], indicating the metastable nature of this phase.

The comparison of the uptake curve for the 2.2 eV

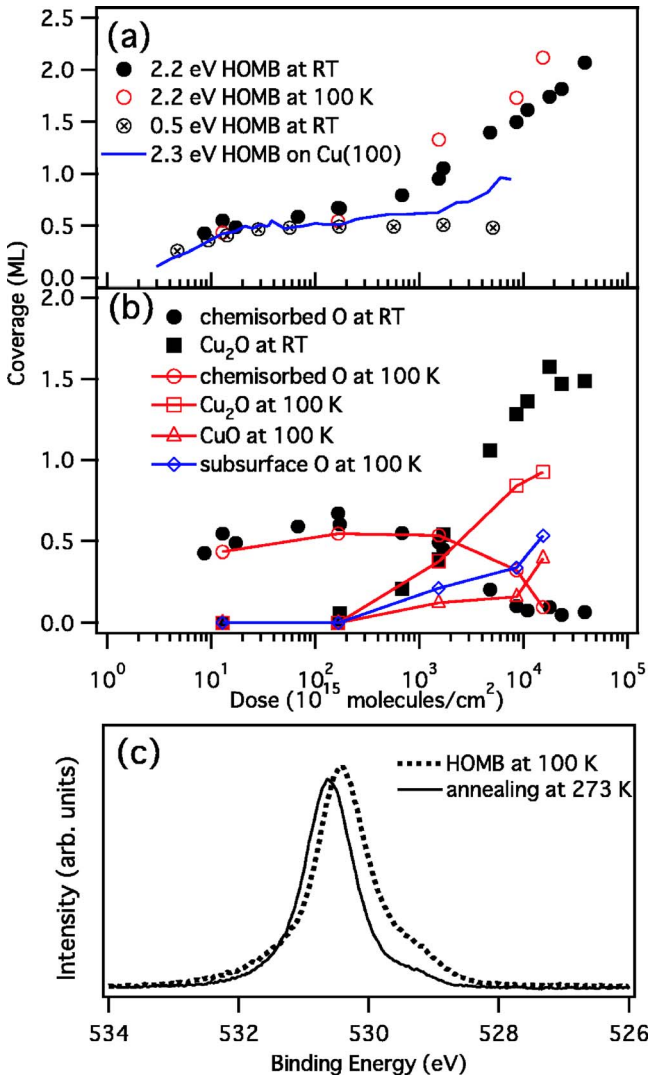

FIG. 4. (Color online) (a) O uptake curves for 2.2 eV HOMB at normal incidence on Cu(410) at room temperature (full circles) and 100 K (open circles). The O uptake at room temperature includes also data recorded at 890.4 eV photon energy. The result for the uptake with 0.5 eV HOMB at normal incidence is also shown. The continuous line shows the corresponding data for Cu(100) (taken from Ref. 19). (b) Uptake curves for chemisorbed O on Cu (530.0 eV, circles), subsurface O (530.1 eV, diamonds), Cu_2O (530.5 eV, squares), and CuO (529.3 eV, triangles) retrieved from the spectra and from the analysis shown in Fig. 2. (c) Comparison between XPS measurements performed immediately after dosing the 2.2 eV HOMB at $T=100$ K (dotted spectrum) and after subsequent annealing (continuous spectrum). The shift witnesses the decreased weight of subsurface O and of CuO.

HOMB deposition with the one at 0.5 eV [reported for comparison in Fig. 4(a)] clearly suggests that higher kinetic energy is required for Cu oxide formation. The CIA mechanism[14] plays, therefore, a role also for the nucleation of the metastable CuO phase, in analogy to the cases of Cu(100) (Ref. 19) and Si(100).[20] The transformation to Cu_2O occurs eventually at higher T when a supply of Cu atoms via diffusion is available. The translational energy of the incident O_2 is thereby used mainly to bury preadsorbed O atoms into

subsurface sites, although local substrate heating may play a role, too.

Fabrication of CuO island at low T is only possible by HOMB. It would be quite interesting to study how the Néel temperature is affected and modified with respect to the bulk value of 229 K,[8] but this is not possible with our experimental setup.

In summary, we demonstrate that nearly perfect Cu_2O films can be grown on Cu(410) by HOMB at room temperature, while also CuO forms at $\sim$100 K. The latter phase disappears when annealing just below RT. This result shows the existence of a reaction route for Cu_2O formation through a metastable CuO precursor when dosing by HOMB on a cold substrate. This process is of general importance for the fabrication of metastable phases of interest for the synthesis of suboxides[32] and of nanostructured materials.[33]

The experiments were performed using SUREAC 2000 in BL23SU at SPring-8 with the approval of the Japan Synchrotron Radiation Research Institute (JASRI) and Japan Atomic Energy Agency (JAEA). The authors are grateful to Y. Saitoh and A. Yoshigoe for their help in operating the monochromatic system at the beamline. The Japanese Ministry of Education, Culture, Sports, Science and Technology is gratefully acknowledged for the Grant-in-Aid for Scientific Research (No. 17550011) that supported this work.

[1] J. R. Waldram, *Superconductivity of Metals and Curprates* (IOP, London, UK, 1996).
[2] P. W. Baumeister, Phys. Rev. **121**, 359 (1961).
[3] F. P. Koffyberg and F. A. Benko, J. Appl. Phys. **53**, 1173 (1982).
[4] J. B. Forsyth, P. J. Brown, and B. M. Wanklyn, J. Phys. C **21**, 2917 (1988).
[5] A. Filippetti and V. Fiorentini, Phys. Rev. Lett. **95**, 086405 (2005).
[6] L. C. Olsen, F. W. Addis, and W. Miller, Sol. Cells **7**, 247 (1982).
[7] G. P. Pollack and D. Trivich, J. Appl. Phys. **46**, 163 (1975).
[8] S. C. Ray, Sol. Energy Mater. Sol. Cells **68**, 307 (2001).
[9] X. G. Zheng, C. N. Xu, K. Nishikubo, K. Nishiyama, W. Higemoto, W. J. Moon, E. Tanaka, and E. S. Otabe, Phys. Rev. B **72**, 014464 (2005).
[10] J. B. Reitz and E. I. Solomon, J. Am. Chem. Soc. **120**, 11467 (1998).
[11] T. Ishihara, M. Higuchi, T. Takagi, M. Ito, H. Nishiguchi, and T. Takita, J. Mater. Chem. **8**, 2037 (1998).
[12] G.-W. Zhou and J. C. Yang, Surf. Sci. **531**, 359 (2003); Phys. Rev. Lett. **93**, 226101 (2004); G.-W. Zhou, W. S. Slaughter, and J. C. Yang, *ibid.* **94**, 246101 (2005).
[13] L. Casalis, M. F. Danisman, B. Nickel, G. Bracco, T. Toccoli, S. Iannotta, and G. Scoles, Phys. Rev. Lett. **90**, 206101 (2003).
[14] L. Vattuone, P. Gambardella, U. Burghaus, F. Cemic, U. Valbusa, and M. Rocca, J. Chem. Phys. **109**, 2490 (1998).
[15] M. Okada, M. Hashinokuchi, M. Fukuoka, T. Kasai, K. Moritani, and Y. Teraoka, Appl. Phys. Lett. **89**, 201912 (2006).
[16] L. Vattuone, L. Savio, and M. Rocca, Phys. Rev. Lett. **90**, 228302 (2003).
[17] E. Vlieg, S. M. Driver, P. Goedtkindt, P. J. Knight, W. Liu, J. Lüdecke, K. A. R. Mitchell, V. Murashov, I. K. Robinson, S. A. de Vries, and D. P. Woodruff, Surf. Sci. **516**, 16 (2002).
[18] J. C. Bouilliard, J. L. Domange, and M. Sotto, Surf. Sci. **8**, 223 (1967).
[19] M. Okada, K. Moritani, S. Goto, T. Kasai, A. Yoshigoe, and Y. Teraoka, J. Chem. Phys. **119**, 6994 (2003).
[20] Y. Teraoka and A. Yoshigoe, Jpn. J. Appl. Phys., Part 1 **41**, 4253 (2002).
[21] http://www.uni-leipzig. de/~unifit/
[22] D. A. Shirley, Phys. Rev. B **5**, 4709 (1972).
[23] M. Okada, A. Gerbi, L. Vattuone, L. Savio, M. Rocca, K. Moritani, Y. Teraoka, and T. Kasai (unpublished).
[24] J. Ghijsen, L. H. Tjeng, J. van Elp, H. Eskes, J. Westerink, G. A. Sawatzky, and M. T. Czyzyk, Phys. Rev. B **38**, 11322 (1988).
[25] A. P. Baddorf and J. F. Wendelken, Surf. Sci. **256**, 264 (1991).
[26] L. H. Dubois, Surf. Sci. **119**, 399 (1982).
[27] Subsurface oxygen on Cu(111) has been identified with an O 1*s* peak at 529.9 eV by J. Bloch, D. J. Bottomley, S. Janz, and H. M. van Driel, J. Chem. Phys. **98**, 9167 (1993).
[28] M. Kauur, K. P. Muthe, S. K. Despande, S. Choudhury, J. B. Singh, N. Verma, S. K. Gupta, and J. V. Yakhmi, J. Cryst. Growth **289**, 670 (2006).
[29] K. P. Muthe, J. C. Vyas, S. N. Narang, D. K. Aswal, S. K. Gupta, D. Bhattacharya, R. Pinto, G. P. Kothiyal, and S. C. Sabharwal, Thin Solid Films **324**, 37 (1998).
[30] M. C. Wu and P. J. Møller, Phys. Rev. B **40**, 6063 (1989).
[31] M. Hirsimäki, M. Lanpimäki, K. Lahtonen, I. Chorkendorff, and M. Valden, Surf. Sci. **583**, 157 (2005).
[32] J. Y. Kim, J. A. Rodriguez, J. C. Hanson, A. I. Frenkel, and P. L. Lee, J. Am. Chem. Soc. **125**, 10684 (2003).
[33] B. Liu and H. C. Zeng, J. Am. Chem. Soc. **126**, 8124 (2004).